

Turbulence Measurements from a Glider

F. Wolk¹*, R.G. Lueck¹, L. St. Laurent²

¹ Rockland Scientific Inc., Victoria, British Columbia, V8Z 1C1, Canada.

² Department of Physical Oceanography, Woods Hole Oceanographic Institution, Woods Hole, MA, 02543-1536, USA

*Corresponding author, e-mail fabian@rocklandsscientific.com

ABSTRACT

To test the feasibility of measuring small-scale turbulence from an ocean glider, a self-contained package carrying velocity shear probes and FP07 thermistors is deployed in a small lake on a *Slocum* ocean glider. The package's turbulence sensors are augmented by a high-resolution pressure sensor and a set of orthogonally mounted accelerometers monitoring the glider's attitude and vibrations. The package is neutrally buoyant and does not limit the glider's manoeuvrability. It attaches to the top of the glider's fuselage with the turbulence sensors positioned just ahead of the glider nose. The package receives power from the glider and can record turbulence data independently for up to 35 days. Data from a test in Ashumet Pond near Cape Cod show that vibration levels of the glider are generally small and do not interfere with the measurement of small-scale turbulence shear. The accelerometer spectra show vibration peaks at 28, 60, and 80 Hz, which are caused by vibrations of the glider's tail fin assembly. These vibrations are stimulated by the action of the glider's buoyancy pump, which acts at the top and bottom turn-around points, and by the action of the rudder, which is activated at regular intervals (~6 seconds) during the flight in order to control the heading of the glider. The vibration peaks have a small magnitude and narrow bandwidth and do not interfere with the shear probe spectrum. The shear probes resolved dissipation rates between $5 \times 10^{-11} \text{ W kg}^{-1}$ in the quiescent layer below the thermocline and $1 \times 10^{-7} \text{ W kg}^{-1}$ in the surface mixing layer. All measured shear spectra fit well with the Nasmyth Empirical Spectrum.

KEYWORDS

Turbulence; shear probes; ocean gliders; mixing

INTRODUCTION

The majority turbulence measurements at dissipation length scales are made using loosely tethered vertical profilers, which are driven by buoyancy and, therefore, provide a nearly vibration-free platform from which to measure the horizontal velocity shear, $\partial u / \partial z$, $\partial v / \partial z$. Lueck *et al.* (2002) give an overview of this “classical” profiler technology. Loosely tethered vertical profilers provide a relatively fast repetition of the measurement, because they can be winched back to the surface at the end of the profile. The tether can also provide a real-time data display, which can guide operational decisions during the experiment. However, the deployment of these profilers requires a considerable amount of experience and skill, as well as dedicated ship time, because it is too risky to operate other over-the-side instrumentation while the profiler is in operation. As a result, the turbulence observations in the world’s oceans remain sparse, despite half a century worth of measurements.

In recent years, the technology of autonomous underwater gliders has matured to provide a new, cost effective infrastructure for observing oceanographic parameters over large areas and over long periods. Approximately 160 commercially available gliders are in operation today, providing measurements of conductivity, temperature, and pressure. Three models of ocean gliders are currently commercially available: The *Slocum Electric Glider* developed by Teledyne Webb Research (Jones and Webb, 2007); the *Seaglider*, developed by the University of Washington (Eriksen *et al.*, 2001); and the *Spray*, developed by Scripps Institute of Oceanography and Woods Hole Oceanographic Institution (Sherman *et al.*, 2001). Similar to ARGO profiling floats, gliders operate by adjusting their buoyancy to move down or up in the water column, while wings and tailfins translate part of the vertical motion into the horizontal component, resulting in a saw-tooth trajectory. Typical vertical-to-horizontal glide ratios are 1:4, resulting in a quasi-vertical, quasi-horizontal measurement. Gliders provide a nearly ideal platform for turbulence measurements because their propulsion does not rely on moving parts, such as propellers, whose vibrations introduce noise into the measured turbulent velocity fluctuations.

Here we present the results from a recent test flight of a *Slocum* glider carrying turbulence shear probes and an *FP07* thermistor. This is the first reported deployment of these sensors on a glider and the data show that the shear probes were able to resolve dissipation rates as low as $5 \times 10^{-11} \text{ W kg}^{-1}$, which is comparable to measurements achieved by the best tethered free-fall profilers. This is encouraging because it shows that gliders are a suitable platform to resolve turbulence levels typically found in the open ocean. The next section describes the instrumentation and experimental setup of the test, followed by a presentation, analysis and discussion of the turbulence data.

INSTRUMENTATION AND EXPERIMENTAL SETUP

Turbulence Package and Glider

The glider is a *Slocum Electric Glider* with a depth rating of 200 m, shown in Figure 1. It has an overall length, including tail fin, of 2.5 m and a hull diameter of 0.21 m. Its mass is 52 kg and the payload capacity is 5 kg. With an alkaline battery pack, the glider's nominal endurance at a 1:4 glide angle and a forward speed of 0.35 m/s is 20 days.

The turbulence package is a *microRider-1000-6* developed by Rockland Scientific Inc. The package is neutrally buoyant and supports two velocity shear probes (Osborn and Crawford, 1980), two *FP07* thermistors, and one SBE7 micro-conductivity probe. These turbulence sensors are mounted on the tapered nose section of the package. Three accelerometers are mounted in an orthogonal configuration on the rear of the pressure bulkhead that separates the nose section from the main pressure housing. The bulkhead also houses the port that connects to a pressure transducer. The main pressure housing contains the signal condition electronics and the data acquisition computer (*Persistor CF2*).

The turbulence package is attached on faired mounting brackets to the top of the glider fuselage, with the turbulence sensors positioned just ahead of the glider nose, outside of the region of flow deformation (Figure 1). In this orientation, the velocity shear probes measure the $\partial w / \partial x$, $\partial v / \partial x$ shear components. The glider/package coordinate system is defined by the orientation of the accelerometers, which, in their nominal configuration, are oriented so that the x -coordinate is forward, y is port, and z is up. The accelerometers pick up a component of gravity and for the given configuration, the glider pitch (θ) and roll (φ) angles are defined as $\theta = \arcsin(a_x/g)$ and $\varphi = \arcsin(a_y/g)$, where g is the gravitational constant and a_x and a_y are

the measured accelerations. Pitch is defined positive when the glider's nose is above the horizontal plane; roll is defined positive when the glider rolls to the left.

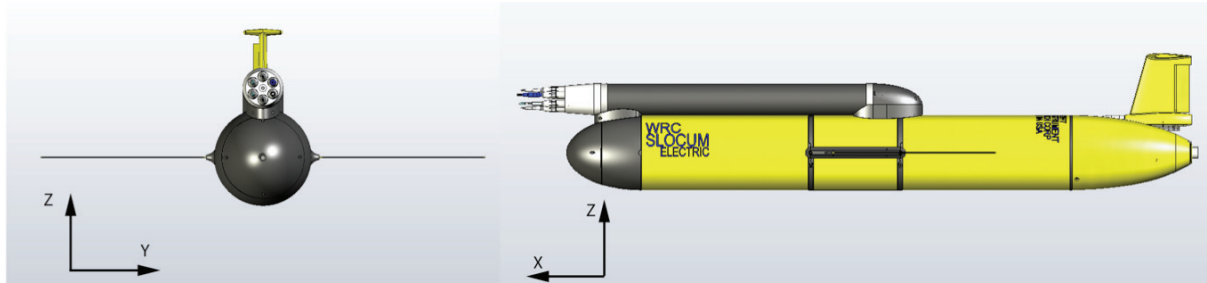


Figure 1: Turbulence package and glider configuration.

Experimental Conditions & Procedures

The test was carried out in Ashumet Pond ($N41^{\circ} 38'2.4''$, $W70^{\circ} 32'5.3''$), a small lake near East Falmouth, MA, which is frequently used by Teledyne Webb Research to test gliders. The lake measures ~ 1350 m north-south by ~ 900 m east-west and has a maximum depth of 20 m. The lack of surface inflow and outflow results in extremely low turbulence levels in the hypolimnion, which makes the lake an ideal site to test the noise level of the glider in terms of the measured dissipation rate.

On the day of the experiment, May 1, 2009, weather conditions were calm with wind speeds less than 5 m s^{-1} and air temperature of 13.5° . The passing of a storm two days prior caused a remnant active surface mixing layer, which was further sustained by convective circulation resulting from latent heat loss to the atmosphere.

Five dives were performed with duration of 500 to 1000 seconds, during which the glider completed between two and four ascent/descent cycles. The glider changes its buoyancy at preset depths by pumping fluid into and out of a cavity. During the ascending and descending portions of the resulting saw tooth path, the glider makes pitch adjustments by shifting the battery pack forward or aft to maintain a straight flight path. During two of the dives (dat_014 and dat_015), this feature was turned off to evaluate the vibrations that result from the battery movement and its possible influence on the shear data. However, due to the absence of large-scale currents in the lake and the relatively short saw tooth cycles, the pitch adjustment was rarely activated. To maintain heading, the glider activates a rudder on the tail fin at regular intervals of approximately 6 seconds. This feature was active in all of the dives.

RESULTS AND DISCUSSION

Glider Attitude and Dynamics

The five separate deployments all gave similar results. Figure 2 shows a summary of the data recorded by the turbulence package during one of the deployments (dat_015). The data are shown after a minimal amount of processing was applied to convert the raw data into physical units. The flight path was a straight line heading west to east, where the glider performed a saw-tooth pattern between 1 m and 12 m depth.

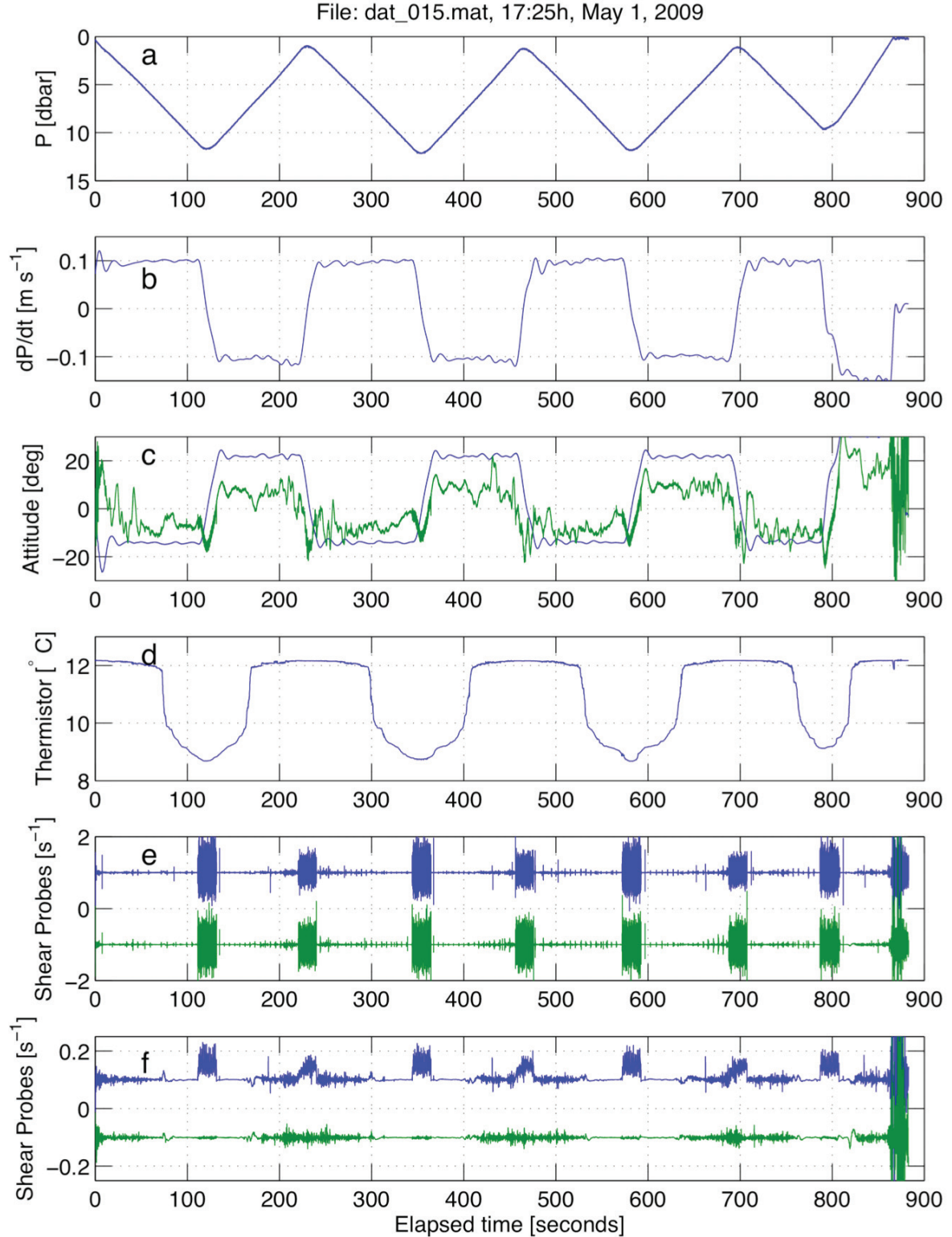


Figure 2: Summary of the data measured by the turbulence package (data file dat_015). All data are shown as elapsed time from the beginning of data file. (a) pressure record; (b) rate of change of pressure, expressed in $\text{dbar s}^{-1} \approx \text{m s}^{-1}$; (c) pitch angle (blue) and roll angle times 10 (green); (d) water temperature measured by the FP07 thermistor; (e) shear probe #1 (blue) and shear probe #2 (green), offset by +1 and -1, respectively; (f) shear probe signals low-pass filtered at 15 Hz.

Three descent-ascent cycles were completed; the fourth cycle starting at 700 s was aborted. The glider's net vertical speed, $W = -dP/dt$, is shown in panel b, and is on average

$9.68 \times 10^{-2} \text{ ms}^{-1}$ ($\sigma = 5 \times 10^{-4}$) during descent and $10.4 \times 10^{-2} \text{ ms}^{-1}$ ($\sigma = 3 \times 10^{-4}$) during ascend. The average pitch angle (panel c) is $-14.1^\circ/22.0^\circ$ during descent/ascent. The pitch angle allows us to estimate the forward speed of the glider along its flight path, $U = W / \sin(\theta)$. Table 1 summarizes the typical speeds and pitch angles observed along the path.

The roll angle is within $\pm 1.5^\circ$. Panel c in Figure 2 shows the roll angle (multiplied by ten). A systematic offset of -27° has been removed from the roll measurement. The offset is the result of misalignment of the turbulence package on the glider.

Table 1. Typical average pitch angle, θ ; vertical speed, W ; and speed along the glide path, $U = W / \sin(\theta)$.

	θ (degrees)	W (m s^{-1})	U (m s^{-1})
Descent	-14.1	-0.096	0.394
Ascent	22.0	0.104	0.280

Angle of Attack

Since the shear probes measure the hydrodynamic lift force created by the turbulent flow, their operation depends on the angle of attack (AOA) of the oncoming flow. Wind tunnel tests with large-scale probe models have shown that the flow over the probe body is laminar for AOA within $\pm 20^\circ$. Outside of this range, the boundary layer separates from the probe and the potential flow theory underlying the operating principle of the probes no longer applies (Osborn and Crawford, 1980).

For the glider, the AOA is the difference between the pitch angle and the angle of the glide path. The manufacturer of the glider states that the average AOA is within $\pm 3^\circ$ during descent and ascent (Teledyne Webb Research, Ben Allsup, personal communication 2009). Simple mathematical models presented by Williams *et al.* (2008) predict an AOA as much as 10° for certain flight conditions. We are in the process of further evaluating the existing data in order to compute the AOA for the glider configuration with the turbulence package used in this experiment. The results of this work will be included in a future presentation.

Vibration Signatures

The possibility of making successful shear probe measurements from the glider depends on the glider's vibration levels, and these were unknown at the onset of this experiment. The shear probes are essentially transverse force sensors and so they are sensitive to rectilinear accelerations. Any vibration of the glider in the 1 to 100 Hz frequency range will show up as a spurious signal in the measured shear signal (Wolk *et al.*, 2002).

An obvious feature in the shear probe signals (Figure 2-e) is vibration contamination when the glider reaches the top and bottom of the saw tooth profile (e.g., at elapsed time 120, 230 s, etc.). The vibrations are caused by the operation of glider's ballast pump, which displaces fluid in order to adjust the buoyancy, but these vibrations are irrelevant. The data at the turning points cannot be interpreted as shear because the forward speed of the vehicle is zero. Additionally, during ascent and descent, numerous smaller vibration signatures are visible at approximately 6-second intervals. These are caused by the glider's rudder, which controls the heading of the glider. The rudder movements are more frequent and stronger at the beginning

of the descent or ascent as the glider accelerates from the turn-around point at the top or bottom of the saw tooth.

Accelerometer spectra (Figure 3) for the x , y , and z directions of the glider (cf, Figure 1) were computed for three conditions: (i) descending glide when neither the buoyancy pump nor the rudder are active (heavy line); (ii) at the bottom of the profile when the buoyancy pump is active (thin solid line); and (iii) descending glide while the rudder is in operation (dotted line).

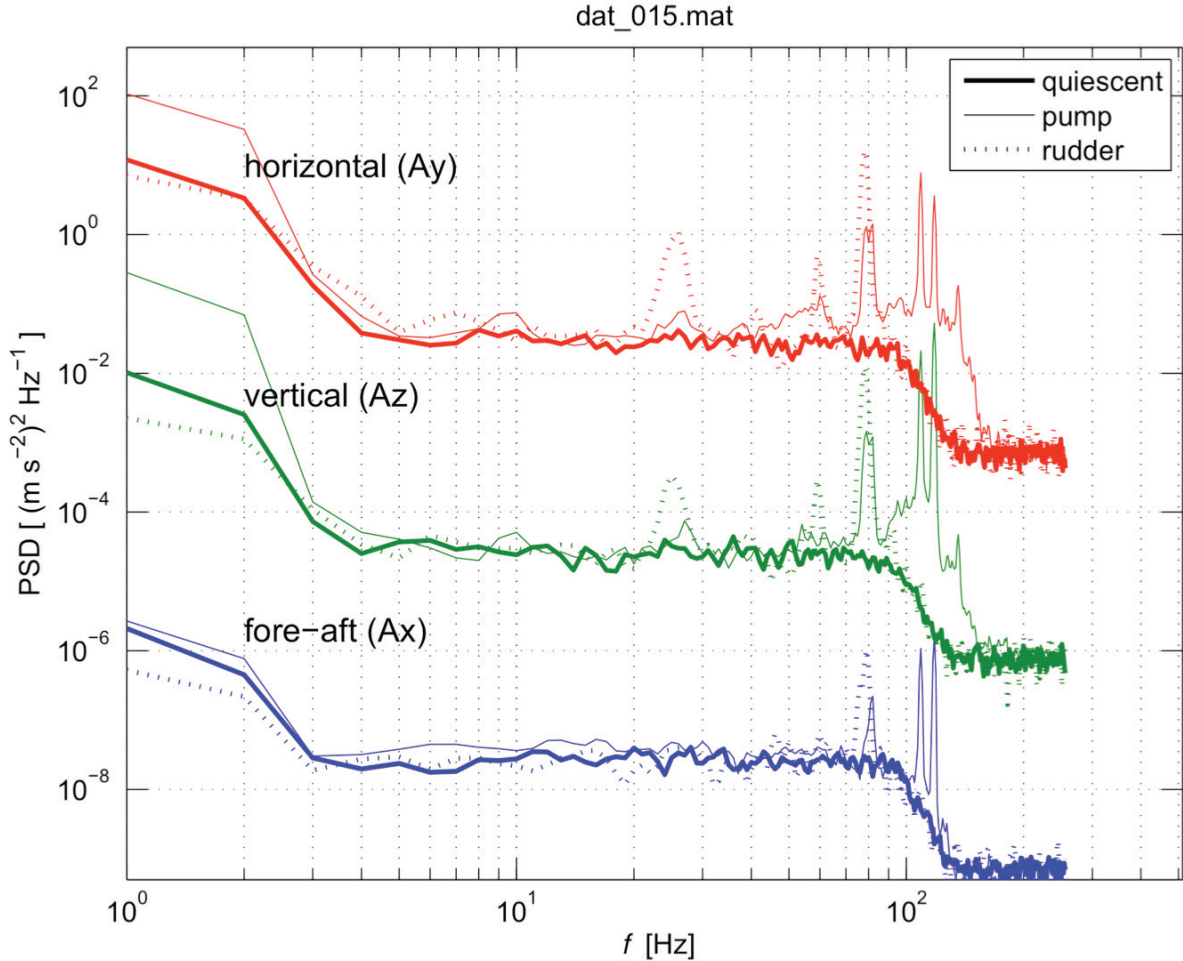


Figure 3: Accelerometer spectra for x -axis (blue), z -axis (green) and y -axis (red) for three conditions: (i) during descent when neither buoyancy pump nor the rudder were active (heavy line); (ii) at the bottom of the profile when the buoyancy pump is running (thin line); (iii) during descent when the rudder is active. The lowest set of spectra is for the x -direction. Spectra for the z - and y -direction are offset by 10^3 and 10^6 , respectively.

For the quiescent condition (heavy line), the spectra are flat throughout the entire frequency band and are at the noise level of the accelerometers. The rise at ~ 1 Hz represents the low-frequency body motions. The anti-aliasing filters suppress the signal variance starting at 98 Hz. The action of the buoyancy pump (thin lines) shows various narrow-banded spectral signatures above 60 Hz. The pump signature is strongest at 80 Hz, with some harmonics at higher frequencies. The vibration signatures are stronger and more broad-banded in the transverse (y , z) directions than in the along-body (x) direction. This is a typical feature of cylindrical bodies, because they are stiffer in the along-axis direction than in the transverse

direction. In the case of the *Slocum* glider, the tail fin, which is mounted on a cantilevered stanchion protruding from the aft of the hull, likely acts as an amplifier for the vibrations. We also note a broader spectral peak centred on 60 Hz in the y direction (horizontal to the glider axis), which is not present in the z component, which is most likely the result of an asymmetry of the glider tail fin, which, by its nature, is more flexible in the y direction than in the z direction.

The action of the rudder (dotted line) shows spectral signatures in the transverse directions at 28, 60, and 80 Hz. The latter corresponds with the 80 Hz vibration excited by the buoyancy pump, and therefore is likely a characteristic frequency of the tail fin assembly. The peak at 60 Hz is more pronounced in the horizontal (y) direction than in the vertical direction (z), because the movement of the rudder is in the x - y plane.

Shear Data

The vibration signatures identified in the accelerometer measurements also show up in the shear data. A segment of data from a descending portion of a dive, between 2.5 m and 11.2 m, is plotted as a “pseudo” vertical profile (Figure 4), showing temperature, temperature gradient, $\partial T_1 / \partial x$, and velocity shear for shear probes #1 and #2, $\partial u_1 / \partial x, \partial u_2 / \partial x$. This representation is practical because it gives a composite view of the measured parameters. It shows small-scale variations along the quasi-horizontal glide path in context with large-scale vertical features. The temperature profile shows a thermocline at ~ 7.5 m depth separating the active surface mixing layer from the quiescent layer below the thermocline. The variance of the temperature gradient and shear signals clearly reflect the different levels of turbulent mixing in the two layers.

The action of the rudder is visible throughout the profile in the unfiltered shear signals (red and green lines). The vibration signature is more pronounced in the $\partial u_1 / \partial x$ signal than in the $\partial u_2 / \partial x$ signal, because the shear probes were orthogonally mounted. The sensitive axis of shear probe #2 was in the horizontal direction, parallel to the movement of the rudder, while the sensitive axis of shear probe #1 was in the vertical direction, perpendicular to the rudder movement. The amplitude of the vibrations decreases over the length of the profile. This is due to the fact that the glider needs to make stronger course corrections at the beginning of the profile, when its speed is slow and the glider is unstable. Similarly, the amplitude of the vibrations signatures is on average larger in the surface mixing layer than in the quiescent layer below the thermocline, because in the turbulence in the surface layer requires stronger rudder action.

In order to reveal the vertical structure in the turbulent velocity, the two rightmost traces in Figure 4 show the shear signals after a 0.15 to 10 Hz band pass filter was applied. The filter effectively removes the high frequency vibration signatures and shows the extremely quiescent conditions below the thermocline. This representation also shows that the shear measurements, on average, have identical signal variance. The single-sided excursion of the shear signals at 7.5 m depth is the result of a pyro-electric effect, which discussed in detail by Lueck (2008). This is a transient effect with a time scale of several 10s of seconds and it occurs when the shear probe’s piezo-ceramic sensing element experiences a change in temperature. The temperature differential can cause an asymmetric expansion of the sensing element, which causes the spurious, transient signal. This effect is most pronounced in large temperature gradients in combination with slow profiling speeds, as is the case here. Because

of the long time scale of the spurious signal, the pyro-electric effect is of no consequence to the shear measurement (Lueck, 2008).

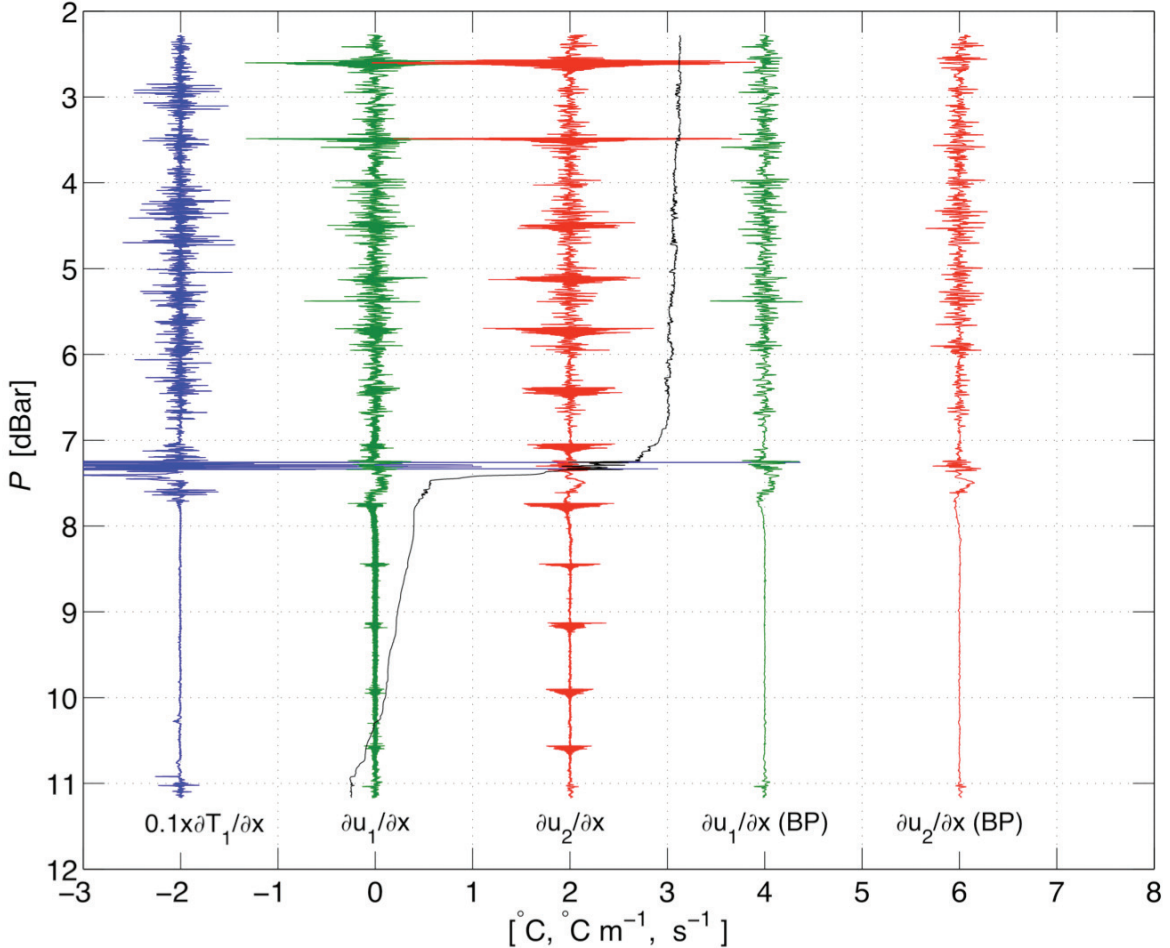


Figure 4: Pseudo profiles of temperature (T_1), temperature gradient ($\partial T_1 / \partial x$), and velocity shear ($\partial u_1 / \partial x, \partial u_2 / \partial x$). Temperature is offset by -9°C . All gradient signals are centred on zero and are offset by integer numbers, as shown. The shear signals $\partial u_i / \partial x, \partial u_2 / \partial x$ are high-pass filtered at 0.15 Hz. The BP labels denote that a 0.15 to 10 Hz band-pass filter has been applied.

Shear spectra were computed for two sections in the turbulent and the quiescent portions of the profile in Figure 4, following the procedure of Goodman *et al.* (2006). The shear signals were high-pass filtered at 0.15 Hz in order to remove low frequency motions of the glider, but this removal of signal content does not affect the calculation of the dissipation rate. For both turbulent and quiescent conditions the measured spectra of both shear probes agree with each other (indicating no systematic biases in the probes' calibration or the electronics of the system) and they agree well with the Nasmyth Empirical Spectrum (hereafter NES; Oakey 1982). Good agreement with the shape of the NES is a measure of the quality of the shear data (Gregg, 1999). The spectra computed from this dive are representative of all other dives that were performed in Ashumet Pond.

The spectra from the turbulent layer (Panel a) were computed from 44 seconds of data. Both spectra for shear probe #1 and shear probe #2 agree with the NES over two decades in wavenumber space, between 1 and 100 cpm. The thin lines are the spectra computed from the

“raw” shear signals ($\partial u_1 / \partial x, \partial u_2 / \partial x$ in Figure 4). The vibration peaks that were identified in the accelerometer spectra are visible in the raw spectra at the higher wavenumbers. For example the peak at 70 cpm corresponds to the 28 Hz peak in the accelerometer data that was associated with the rudder action. Other vibration peaks at higher wavenumbers can be similarly matched with the accelerometer data. Note, however, the vibration peak in the shear probe #1 spectrum at 100 cpm, which corresponds to a frequency of 40 Hz. At this frequency the accelerometer spectra show only a very small vibration signature. The reason is that the shear probes are mounted in front of the pressure case and they tend to amplify vibrations because of the leveraging effect of their protracted position.

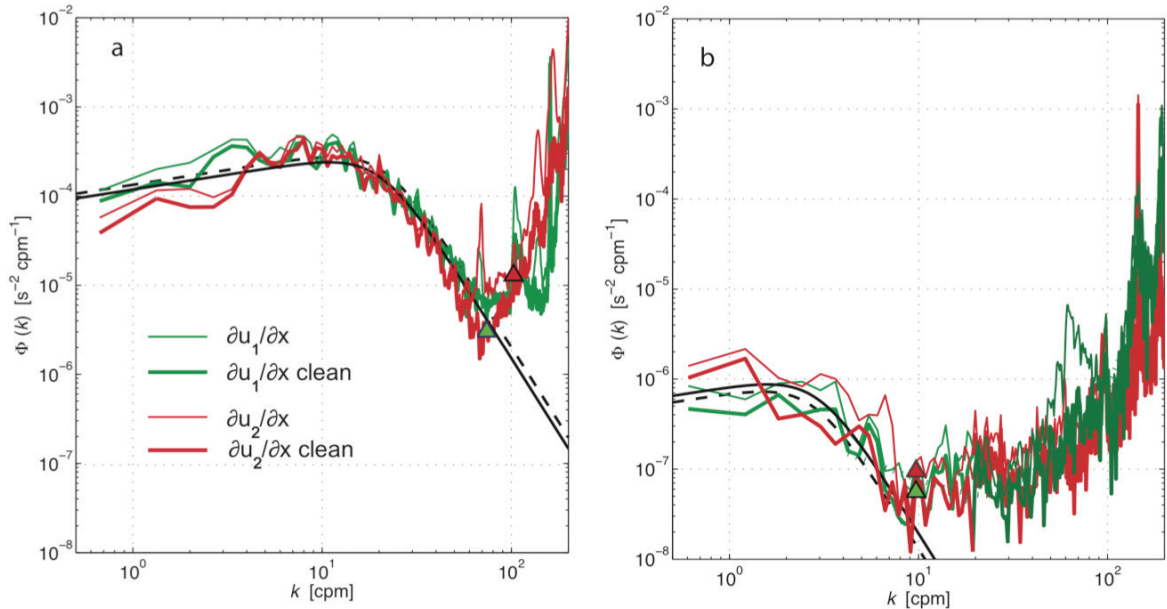


Figure 5: Shear spectra computed from the turbulent surface layer (a) and the quiescent bottom layer (b). Green lines are from shear probe #1 and red lines are from shear probe #2. The thin lines are the spectra computed from the “raw” shear signals, where only a 0.15-Hz high pass filter was applied to remove low-frequency (large scale) motions of the glider. The heavy lines are spectra after signal content coherent with the accelerometer data was removed from the shear signals using the Goodman Method (Goodman *et al.*, 2006). The triangles denote the wavenumber cutoff points used in the computation of the dissipation rates.

The vibration signatures can be very effectively removed from the shear probe data by using the information from accelerometers. This technique was first suggested by Levine and Lueck (1999) and later refined for three dimensions by Goodman *et al.* (2006). By calculating the three-dimensional coherence matrix between a shear probe signal and the (three) accelerometer signals, only signal content that is coherent with that of the accelerometers (i.e., caused by body vibrations) is removed. The “clean” shear spectra are shown as the heavy lines in Figure 5. After this treatment, the dissipation rates are computed from the cleaned shear spectra using

$$\varepsilon = 7.5\nu \int_0^{k_{\max}} \Phi(k) dk ,$$

where ν is the kinematic viscosity and k_{\max} is the maximum wavenumber of integration, indicated by the triangular markers in the figure. For shear probe #1 $\varepsilon_1 = 6.8 \times 10^{-8} \text{ W kg}^{-1}$ with

a viscous cutoff wavenumber (Kolmogorov wavenumber) of $k_v = 81 \text{ cpm}$; and for shear probe #2 $\varepsilon = 5.8 \times 10^{-8} \text{ W kg}^{-1}$ with $k_v = 78 \text{ cpm}$. Note that the vibration peaks are above the viscous cutoff wavenumber, so that the shear spectra are fully resolved.

The spectra from the quiescent layer also show good agreement with the NES. These spectra were computed from only a 16-second segment of data, and so they exhibit a higher statistical uncertainty. Dissipation rates computed for the two shear probes are $\varepsilon_1 = 2.5 \times 10^{-11} \text{ W kg}^{-1}$ with $k_v = 11 \text{ cpm}$ and $\varepsilon = 3.3 \times 10^{-11} \text{ W kg}^{-1}$ with $k_v = 12 \text{ cpm}$. Again, it is worthwhile to note that while the vibration peaks are visible at the higher wavenumbers, none of the noise peaks falls into the wavenumber range of the turbulent shear spectrum. This shows that the glider has extraordinarily low noise levels, which means that the glider can resolve open ocean turbulence levels.

CONCLUSIONS

Data were presented from the first test flight of a *Slocum* glider carrying a turbulence sensor package with velocity shear probes. The test was carried out in a small lake, which provided a practical test location. The lake did not have any strong currents and very low turbulence levels below the thermocline, which made it possible to assess the noise level of the glider in terms of the measured dissipation rate of turbulent kinetic energy.

Three main results from these tests are:

- The flight dynamics of the *Slocum* glider were not negatively affected by the presence of the turbulence package. Typical vertical speeds of the glider were 0.1 m s^{-1} , which corresponded to 0.4 m s^{-1} of forward speed along the glide path. This is a nearly ideal speed from shear probe measurements.
- The glider's sources of vibration noise are the ballast pump, battery shifting for pitch control, and the rudder action for course control. The pump noise is significant but it occurs only at the turn-around points of the saw tooth profile and, therefore, is irrelevant for the shear probe measurements. The noise resulting from the battery shifting was not detectable in this test. The noise from rudder action occurs at high wavenumbers and does not affect shear measurement.
- Dissipation rates from $\sim 10^{-7} \text{ W kg}^{-1}$ in the surface mixing layer of the lake down to $\sim 5 \times 10^{-11} \text{ W kg}^{-1}$ below the thermocline were measured. This shows that the glider matches the performance of the best vertical profilers in terms of the resolved dissipation rate.

Future work will be directed towards assessing the angle of attack, which is the difference between the glider's pitch angle and its glide path. More tests will be carried out to assess the additional drag introduced by the turbulence package, in order to estimate the impact on the glider's power consumption and endurance.

Acknowledgements: Ben Allsup and Peter Collins of Teledyne Webb Research and Ken Decoteau of FSU supported the fieldwork at Ashumet Pond. The glider and microstructure work of LS is supported by the US Office of Naval Research Physical Oceanography Program. The instrument system described here was funded through ONR contracts N00014-05-1-0360 and N00014-09-1-0289.

REFERENCES

- Eriksen, CC, T.J. Osse, R.D. Light, T. Wen and T.W. Lehman (2001). Seaglider: A long-range autonomous underwater vehicle for oceanographic research. *IEEE Journal of Oceanic Engineering*, **26**, 424–436.
- Gregg, M.C., 1999: Uncertainties and Limitations in Measuring ε and χ . *T. J. Atmos. Oceanic Technol.*, **16**, 1483–1490.
- Goodman, L., E.R. Levine and R.G. Lueck (2006). On Measuring the Terms of the Turbulent Kinetic Energy Budget from an AUV. *J. Atmos. Ocean. Tech.*, **23**, 977–990.
- Jones, C. and D. Webb (2007). Slocum Gliders, Advancing Oceanography. In: *Proceedings of the 15th International Symposium on Unmanned Untethered Submersible Technology conference (UUST'07)*, Durham, NH, USA, 19 to 20 August 2007. Autonomous Undersea Systems Institute.
- Levine, E.R., and R.G. Lueck (1999): Turbulence Measurement from an Autonomous Underwater Vehicle. *J. Atmos. Oceanic Technol.*, **16**, 1533–1544.
- Lueck, R. (2008). Testing of the EAWAG VMP-500-028 in Harry Lake. Application Note AN-017, Rockland Scientific Inc., Victoria, B.C., Canada. Available at <http://www.rocklandsscientific.com> (July 2009) or through info@rocklandsscientific.com.
- Lueck, R., F. Wolk, and H. Yamazaki (2002). Oceanic velocity microstructure measurements in the 20th century, *J. Oceanography*, **58**, 153 – 174.
- Oakey, N. (1982). Determination of the Rate of Dissipation of Turbulent Energy from Simultaneous Temperature and Velocity Shear Microstructure Measurements. *J. Phys. Oceanogr.*, **12**, 256–271.
- Osborn, T. R., and W. R. Crawford (1980). An airfoil probe for measuring turbulent velocity fluctuations in water. *Air–Sea Interaction: Instruments and Methods*, L. H. F. W. Dobson and R. Davis, Eds., Plenum, 369–386.
- Sherman, J., R.E. Davis, W.B.Owens and J.Valdes (2001). The autonomous underwater glider Spray. *IEEE Journal of Oceanic Engineering*, **26**, 437–446.
- Williams, C.D., R. Bachmayer and B. deYoung (2008). "Progress in Predicting the Performance of Ocean Gliders from At-Sea Measurements", Proceedings of the OCEANS'08 MTS/IEEE, September 15 to 18, 2008, Québec City, Québec, Canada.
- Wolk, F., H. Yamazaki, L. Seuront, and R. Lueck (2002). A new free-fall profiler for measuring biophysical microstructure. *J. Atmos. Ocean. Tech.*, **19** (5), 780–793.